

physically reasonable simplification is needed.

One way of making the rate calculation practicable is to reduce the problem to one dimension. The first such attempt was made in the absolute rate calculation of proton migration in the enol-form malonaldehyde.⁴² We can imagine a picture of a large-amplitude nuclear motion in which the reacting system proceeds along the IRC with normal vibrational motions in the plane perpendicular to the direction of IRC. We assume in this approximation a "vibrational adiabaticity"⁴³ with regard to the large amplitude "translational" motion along the IRC.

The result⁴² for malonaldehyde proton migration did not agree with experiment, although the adiabatic approach illustrated the one-dimensional reduction. The rate constant obtained ($\sim 10^{14} \text{ s}^{-1}$) was 10^2 – 10^3 times larger than that estimated from experimental studies ($\sim 10^{11} \text{ s}^{-1}$). Obviously, this result was partially caused by the small potential barrier, less than 1 kcal/mol, adopted in the calculation. The numerical result could have been no doubt improved by taking the barrier height to be 11 kcal/mol which was recently obtained by theoretical calculations.⁴⁴ Such a presumption is actually ascertained by a simpler tunneling calculation.^{12a}

The Hamiltonian valid for a narrow region along the IRC is called the IRC Hamiltonian. The effect of vibrational nonadiabaticity⁴⁵ can be taken into account

(42) S. Kato, H. Kato, and K. Fukui, *J. Am. Chem. Soc.*, **99**, 684 (1977).

(43) R. A. Marcus, *J. Chem. Phys.*, **43**, 1598 (1966); **46**, 959 (1967); M. Quack and J. Troe, *Ber. Bunsen ges. Phys. Chem.*, **78**, 240 (1974); **79**, 170 (1975).

(44) G. Karlström, H. Wennerström, B. Jönsson, and S. Forsén, *J. Am. Chem. Soc.*, **97**, 4188 (1975); E. M. Fluder and J. R. de la Vega, *ibid.*, **100**, 5265 (1978); J. Catalán, M. Yáñez, and J. I. Fernández-Alonso, *ibid.*, **100**, 6917 (1978).

in the IRC Hamiltonian. A calculation of the tunneling rate of the reaction $\text{HNC} \rightarrow \text{HCN}$ was carried out^{46a} by the use of the IRC Hamiltonian of Miller and co-workers,^{46b} obtaining the interesting result that the rate constant value $\sim 10^5 \text{ s}^{-1}$ was achieved about 8 kcal/mol below the classical threshold.

Concluding Remarks

The IRC approach in chemodynamical studies has just begun to take shape. The present stage of the theory is mainly to establish a framework. With this in mind the theory has been formulated to be as broadly applicable as possible. At this stage, it may be tolerable to sacrifice pragmatism because of the shortage of efficient computing procedures. It is expected that in the near future, however, actual calculations will become feasible using a new generation of computers. In anticipation of these advances, the theory should be armed with mathematical foundations.

In particular, the *global* character of configuration space should be clarified by the use of global coordinates. The solution of the multidimensional Schrödinger equations, the rate problem in general nonadiabatic cases, the intercell tunneling rate involving infinite cells, the treatment of the nonzero angular momentum case using the general kinetic energy formula of eq 11, and IRC approach for excited state reactions, and so forth will be explored by mathematical methods.

It is a pleasure to acknowledge the reviewers of the manuscript and the editors for their suggestions and comments.

(45) R. A. Marcus and M. E. Coltrin, *J. Chem. Phys.*, **67**, 2609 (1977); R. A. Marcus, *J. Phys. Chem.*, **83**, 204 (1979).

(46) (a) S. K. Gray, W. H. Miller, Y. Yamaguchi, and H. F. Schaefer, III, *J. Chem. Phys.*, **73**, 2733 (1980); (b) W. H. Miller, N. C. Handy, and J. E. Adams, *ibid.*, **72**, 99 (1980).

The Semiclassical Way to Molecular Spectroscopy

ERIC J. HELLER

*Department of Chemistry, University of California, Los Angeles, California 90024,
and Los Alamos National Laboratory, Los Alamos, New Mexico 87545*

Received June 22, 1981

This Account deals with a new perspective on the interaction of light with molecules. Although much of chemistry may take place in the dark (literally and figuratively), our knowledge of fundamental molecular and chemical processes is often greatly enhanced when we shed light on the subject! Light of various wavelengths and intensities can be used as a probe of molecular structure and dynamics, and sometimes light acts as a reagent or product in a chemical reaction.

Very often, we can profit from a classical or semiclassical picture of the interaction of light with molecules. It is easy, for example, to imagine a heteronuclear

diatomic molecule as two partially charged masses connected by a spring, oscillating and absorbing energy due to a resonantly oscillating electric field. This picture enhances our understanding of infrared vibrational transitions.

In electronic absorption and emission spectra, we also have a classical picture of sorts, namely, the Franck-Condon idea of a vertical transition in which the sluggish nuclei retain their position and momentum while the electrons quickly make a transition. After the electrons have made a transition, the nuclei experience new forces; they find themselves displaced relative to the equilibrium geometry of the new potential surface, and interesting dynamics should ensue. Unfortunately, most discussions of electronic transitions cut short any allusions to dynamics and explain the absorption spectrum in terms of Franck-Condon overlaps of the

Eric Heller is Professor of Chemistry at University of California, Los Angeles. He received his B. S. degree from the University of Minnesota in 1968 and the Ph.D. at Harvard University in 1973, with W. P. Reinhardt. He joined the faculty at UCLA following 2 years of postdoctoral work with S. A. Rice at the University of Chicago.

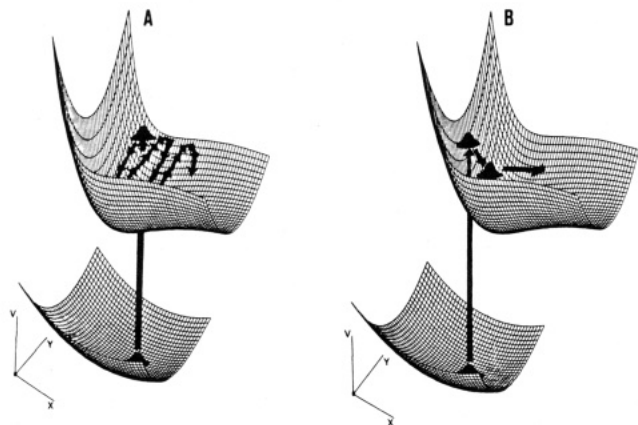


Figure 1. (A) Photoabsorption between two Born–Oppenheimer potential surfaces. The Franck–Condon wave packet $\phi(t)$, arising out of $\phi = \mu\chi$ (χ is shown on the lower surface, ϕ and $\phi(t)$ on the upper), takes a circuitous path in this case, “grazing” $\phi(0)$ several times on the way to dissociation. The result is an absorption band with some low-resolution vibrational structure. (B) Direct dissociation leading to a broad, featureless absorption band.

initial nuclear wavefunction with a time-independent vibrational *eigenfunction* of the upper electronic potential surface. We (and the nuclear wave function) are left hanging; we are given no explanation of the time evolution of the hapless nuclei which, once the photon is absorbed, are ready to move in ways that *determine* the spectra.

What happens to the nuclei, in an internal coordinate picture, is depicted in Figure 1. The initial nuclear wave function is really a localized *wave packet*, being typically a ground or low-lying vibrational state. The packet slides downhill, following at first the path of steepest descent, changing shape (see Figure 1). This path very closely approximates a classical path, at least for a few vibrational periods. The wave packet dynamics corresponds to some specific vibrational motion that can be visualized in terms of bond distances, angles, etc. How the wave packet dynamics determine electronic and Raman spectra and the intuitive and computational advantages of this picture are the subjects of this Account.

The need to understand and predict the spectra of large isolated molecules places the theorist in an awkward position. On the one hand, rules or “recipes” for calculating spectra have been known for 50 years or more. On the other, the ingredients (wave functions, energies, matrix elements, etc.) that go into the recipes are virtually impossible to calculate for large molecules. Putting aside the question of finding potential surfaces, there is no present or foreseeable computer that will allow the determination of vibration–rotation eigenstates when the density of states is 10^5 to 10^{14} per wavenumber, a not uncommon situation.

Fortunately, our needs shift from having to know individual transition probabilities in small molecules (or large molecules at very low energy) to having to understand spectral *features* in larger molecules at moderate energies which may be composed of thousands or trillions of individual transitions. Thus, if we cannot determine the matrix element of the dipole μ ,

$$\mu_{0k} = \langle \psi_0 | \mu | \psi_k \rangle \quad (1)$$

because ψ_k is one state (with 26 coordinates, say) of 10^9 per cm^{-1} , we can take solace in the knowledge that μ_{0k}

will never be measured! However, a somewhat smoothed absorption spectrum *is* measurable, and a recipe is

$$\epsilon(\omega) = \eta\omega \sum_k \Delta(\omega - \omega_k) |\mu_{0k}|^2 \quad (2)$$

where $\Delta(\omega - \omega_k)$ is a function peaked at $\omega = \omega_k$ and η is a constant. Now, the recipe (eq 2) seems straightforward enough, but the ingredients are far too exotic. To predict an electronic absorption spectrum may easily require 10^{10} or more μ_{0k} 's, each of which we cannot compute! How then do we compute the absorption spectrum?

A hint as to how to proceed is provided with analogy to a branch of spectroscopy that long ago abandoned the idea of dealing with eigenstates of the total system. In the spectroscopy of condensed phases, a manifestly time-dependent approach is adopted. Spectra are formulated in terms of Fourier transforms of appropriate autocorrelation functions. For example, the infrared absorption spectrum is given by¹

$$I(\omega) = \frac{c}{2\pi} \int_{-\infty}^{\infty} dt e^{i\omega t} \langle \mu(0)\mu(t) \rangle \quad (3)$$

where c is a simple known function of frequency and where the brackets imply an average over the density matrix ρ for the entire system. The “system” may be anything from a small molecule in a pure quantum state to a large ensemble of molecules at finite temperature. In the latter situation, the time-dependent nature of eq 3, together with the expectation that finite temperatures will wash out many quantum effects, has led to time-dependent classical and semiclassical approaches for finding the spectra. For example, Berens and Wilson² perform classical molecular dynamics calculations with a few simple quantum corrections and evaluate eq 3 for diatomic molecules in condensed media. Koszykowski and Marcus³ use an approximate classical binary collision approach to calculate the autocorrelation function. In a study closer in spirit to ours, Lax⁴ examined spectra of solids. There is a large literature on the autocorrelation approach to spectra, much of it based in one way or another on classical mechanics. The lesson is that, when there are enough degrees of freedom, *adopt a time-dependent approach and implement it classically or semiclassically.*

The same conclusion, at least as regards the desirability of a time-dependent formulation, can be reached by considering the spectrum of a typical large molecule. Experimental conditions or extreme congestion of levels may render the spectrum featureless on a scale of less than 10 to 100 wavenumbers. This corresponds, via the Uncertainty Principle, to 1–0.1 ps. Thus, if we write down the correct time-dependent expression for the spectrum, we shall have to evaluate it for less than a picosecond to predict the spectrum to the available resolution. Very often, much broader spectral features are of interest, and, for example, the broad Franck–Condon envelope of an electronic transition can typically be obtained with 1–5 fs worth of dynamics! In many such spectra, especially in electronic transitions

(1) R. G. Gordon, *Adv. Magn. Reson.*, **3**, 1 (1968).

(2) P. H. Berens and K. R. Wilson, *J. Chem. Phys.*, **74**, 4872 (1981).

(3) M. L. Koszykowski and R. A. Marcus, *J. Chem. Phys.*, **68**, 1216 (1978).

(4) M. Lax, *J. Chem. Phys.*, **30**, 1752 (1952).

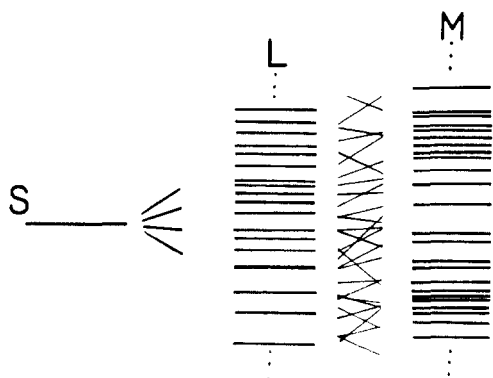


Figure 2. A typical "states and ladders" setup, with an initially excited state, S , and two manifolds, $\{L\}$ and $\{M\}$.

with a drastic change in potential (e.g., charge transfer, photodissociation, or photoelectron spectra), the broad envelope is often all that is observable.

Once we have reformulated various intramolecular spectroscopies in a time-dependent, fully quantum-mechanical way, we have far more palatable recipes for calculating spectra for large molecules. Most often, we find ourselves compromising a bit on the ingredients by using semiclassical input dynamics. If the semiclassical method should prove insufficient, the next step of time-dependent variational approaches⁵ is still far easier than finding eigenfunctions.

There are two great advantages to a semiclassical approach to molecular spectra. First, we all acquire some classical intuition born of experience in the ordinary world. Refinement of this intuition through the explicit study of classical mechanics is reviving, with the recently added features of computer simulations and graphics. The second advantage has to do with a tremendous surge of interest in classical dynamics among astronomers, physicists, and now chemists, spurred and accompanied by a new qualitative understanding of the dynamics of complicated nonlinear systems (e.g., molecules!).⁶ This new qualitative understanding has been greatly aided by the advent of large, fast computers. Much of the recent, purely classical work on the stability of motion of dynamical systems and the question of the onset of stochasticity or chaotic motion in these systems is directly relevant to molecular spectroscopy and intramolecular dynamics.

Before proceeding to specific insights and new techniques for molecular spectroscopy and dynamics, provided by our semiclassical time-dependent approach, we mention a class of related and much better known time-dependent methods known under various names such as Green's function approach, Bixon-Jortner method, level coupling methods, etc. These techniques are all time dependent, but not semiclassical. Such methods, which we call "states and ladders", are in our opinion often only partially successful in overcoming the problems of high density of states in large molecules. Let us consider Figure 2, which shows a typical setup in the states-and-ladders approach. A spectroscopically populated state $|S\rangle$ is coupled to states $\{|L\rangle\}$ which are further coupled to states $\{|M\rangle\}$. The M -manifold is a ladder for the states $\{|L\rangle\}$, which in turn is a ladder for the state $|S\rangle$.

(5) E. J. Heller, *J. Chem. Phys.*, **64**, 63 (1976).

(6) R. G. Helleman in "Fundamental Problems in Statistical Mechanics", Vol. 5, E. G. D. Cohen, Ed., North Holland, New York, 1980.

First, let us discuss the successes of the states-and-ladders approach. (1) It is completely general. Any molecule can, in principle, be described in this way. (2) It is quite successful at *qualitatively* explaining decay of prepared states, buildup and decay of the ladders, etc. (3) When something is really known about the levels and their couplings, the states-and-ladders method can be extremely useful in understanding the flow of probability in the molecule.⁷

The disadvantages, in our opinion, of the states-and-ladders method are (1) most often the states, ladders, and especially the couplings between them are poorly known and poorly understood. The extreme generality of these methods, together with the lack of knowledge about the quantities that go into them, is a dangerous combination. Many phenomena can be formally "explained" with precious little specific input information. (2) Even if the states and couplings are known, the resulting time dependence expressed in terms of the states may be extremely complicated, even though the molecule may really be doing something quite simple when viewed in another picture.

We hope that, after reading the following, the reader will agree that the semiclassical time-dependent method is indeed "another picture" that can provide a great deal of insight and predictive power for the intramolecular dynamics relevant to several types of spectroscopy.

Time-Dependent Formulation

Photoabsorption Formula. Here, we give the recipes for electronic absorption and emission, and later, for Raman scattering. Our general approach is aimed at subsequent semiclassical implementation and the recipes, though simple and *exact within the Born-Oppenheimer approximation*, are perhaps unfamiliar. Derivations may be found in ref 8-12, but for now the reader is simply asked to believe the recipes and share in the fun of understanding their implications.

Consider Figure 1A. Here, we show two Born-Oppenheimer potential surfaces, each relevant to two vibrational degrees of freedom, x and y . Shown also in the ground-state vibrational wave function χ and vertically above it, with an arrow representing the photoabsorption, the wavefunction ϕ which is simply

$$\phi(x,y) = \mu(x,y)\chi(x,y) \quad (4)$$

The electronic transition moment μ between the two surfaces is a function of coordinates often taken to be a constant in the Condon approximation. "Upstairs", ϕ is not a stationary state; it is a displaced wave packet, and it will evolve as $\phi(t)$ according to the time-dependent Schrödinger equation

$$i\hbar \frac{\partial \phi(t)}{\partial t} = H\phi(t) \quad (\phi(0) \equiv \phi) \quad (5)$$

where H is the vibrational Hamiltonian for the upper surface. The absorption spectrum is then given by^{9,10}

$$\epsilon(\omega) = C\omega \int_{-\infty}^{\infty} e^{i(\omega+E_0)t} \langle \phi | \phi(t) \rangle dt \quad (6)$$

(7) H. W. Galbraith and J. R. Ackerhalt, "Theoretical Treatment of Collisionless Multiphoton Excitation in SF_6 ", to be published.

(8) E. J. Heller, *J. Chem. Phys.*, **62**, 1544 (1975).

(9) E. J. Heller, *J. Chem. Phys.*, **68**, 2066 (1978).

(10) E. J. Heller, *J. Chem. Phys.*, **68**, 3891 (1978).

(11) K. C. Kulander and E. J. Heller, *J. Chem. Phys.*, **69**, 2439 (1978).

(12) S.-Y. Lee and E. J. Heller, *J. Chem. Phys.*, **71**, 4777 (1979).

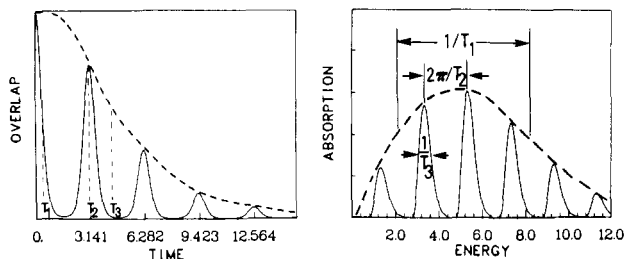


Figure 3. (Left) Absolute value of $\langle \phi | \phi(t) \rangle$ for the case of Figure 1B. Three important time scales, T_1 , T_2 , and T_3 , are shown. (Right) Spectrum arising out of Figure 1A and the autocorrelation function. Note how T_1 , T_2 , and T_3 affect the spectrum.

where C is a constant, ω is the frequency of incident radiation, and E_0 is the energy of χ . Thus, the overlap of $\phi(t)$ with ϕ , Fourier transformed, gives the spectrum. Once $\langle \phi | \phi(t) \rangle$ is known, all frequencies are trivially obtainable. (Emission is treated the same way, with ω^3 replacing ω in eq 6 and the roles of the upper and lower surfaces reversed.)

Where could the Franck–Condon principle be better displayed than in eq 6? Equation 6 helps to cast away doubts about the instantaneous nature of the electronic transition relative to the actual slow arrival of the light impinging on the molecule: the spectrum at frequency ω is the Fourier transform of the dynamics following an instantaneous Franck–Condon transition at $t = 0$. The instantaneous transition could be effected with a very short light pulse. If lingering doubts exist about what “really happens” in the laboratory, the derivation given by Kulander and Heller¹¹ shows that, while the laser of frequency ω is turned on, “little pieces” of the ground-state wave function are constantly being brought upstairs (with phase $e^{i\omega t}$) while the pieces already upstairs are functionally just $\phi(t)$ at various times t . As these pieces return to their birthplace, new pieces are still coming up, constructively (or destructively) interfering with the old pieces and causing absorption maxima (or minima).

Spectral Features and Dynamics. Now we can understand a great deal, in physical terms, about the absorption spectrum arising out of the situation depicted in Figure 1A. The spectrum is shown in Figure 3 (right). The maximum in the absorption envelope (dashed line) has long been known to be close to the vertical distance to the upper potential surface measured from the Franck–Condon vicinity of the state χ . But what about the width of the envelope? By the time-energy Uncertainty Principle, this broadest feature of the spectrum, its width, comes from the shortest feature in time. This feature is the initial decay in the overlap $\langle \phi | \phi(t) \rangle$ (Figure 3, left), caused by the movement of $\phi(t)$ directly downhill along the path of steepest descent. This falloff is very nearly Gaussian for large displacements, and if we assign it a standard deviation T_1 , then the standard deviation of the resulting Gaussian envelope is $\Delta\omega = 1/T_1$. The trajectory of the quantum packet $\phi(t)$ is almost exactly classical for short times if we compute the expectation values

$$x_t = \langle \phi(t) | x | \phi(t) \rangle \equiv \langle x \rangle_t$$

$$p_{xt} \equiv \langle p_x \rangle_t \quad (7)$$

and compare with the trajectory. In fact, Ehrenfest’s theorem tells us this should be the case. Clearly, the steeper the upper surface in the Franck–Condon region,

the faster the decay in $\langle \phi | \phi(t) \rangle$ and the broader the absorption envelope. Anything that happens at longer times can only add increasingly detailed structure to the spectrum, but it cannot change the envelope of the spectrum.

After the initial falloff in $\langle \phi | \phi(t) \rangle$, the overlap stays low until $t \approx T_2$, when the wave packet returns to the vicinity of its birthplace, as shown in Figure 3 (left) and Figure 1A. The “grazing collision” of $\phi(t)$ with ϕ causes a bump in the overlap at $t \approx T_2$. Since $\phi(t_2)$ is displaced and spread relative to ϕ , the overlap obeys $|\langle \phi | \phi(t_2) \rangle| < |\langle \phi | \phi(0) \rangle|$. Subsequent bumps of progressively lower amplitude may occur. The recurrences in the time domain, spaced by time T_2 , cause structure in the frequency domain spaced by $2\pi/T_2$ (Figure 3, right).

The final outcome of the packet in our example is dissociation. This means that the progressive decay in the peak overlap is permanent, and unresolvable broadened lines result in the spectrum. The frequency deviation σ_ω of the lines, assuming a Gaussian damping of the subsequent overlap peaks (dashed line in Figure 3, left), is $1/T_3$.

We have now begun to understand spectral features in terms of physical wave packet dynamics. As another example, the reader can perhaps see that, if the Franck–Condon region had been as seen in Figure 1B, the spectrum would have been broader than in Figure 3 (right) (the potential is steeper) and structureless. Figure 1B corresponds to a direct dissociation, Figure 1A to a “vibrational predissociation”.

If we start with an initially excited vibrational wave function χ , some interesting effects arise which also succumb easily to the same time-dependent formalism. For example, in one dimension, the absorption spectrum out of an eigenstate usually “reflects” the nodal structure of that state: we get one large “bump” in the envelope for absorption out of the ground state, two bumps for the first excited state, and so on. This is not always true in two or more dimensions. It depends on whether the nodes in the wave function ϕ are parallel or perpendicular to the downhill direction on the upper surface. If the nodal surfaces are perpendicular to the downhill direction, they will be seen in the absorption spectrum as low-resolution bumps. If parallel, they will be silent in the spectrum. This can be seen from a slightly more detailed consideration of the time dependence and the modifications that the nodal structure introduces. It can also be seen with the aid of the multidimensional reflection approximation, first derived in ref 9.

It is not hard to see, from formula 6, why large molecules very often have smooth, almost structureless, absorption spectra. In order for structure in the spectrum to appear, there must be at least a partial recurrence in $\langle \phi | \phi(t) \rangle$ within a picosecond or so after the initial decay. After a picosecond, the resulting absorption structure caused by a recurrence will likely be washed out by rotational band contours, solvent effects, etc. For the recurrence to occur, all atoms in the molecule must return *simultaneously* to near their starting positions. Even one out of place will “kill” $\langle \phi | \phi(t) \rangle$, for this overlap involves all the coordinates. For a large molecule, certain factors can nonetheless cause a recurrence: (1) the displacement is small in the

excited state, so $\langle \phi | \phi(t) \rangle$ has very little space in which to wander; (2) symmetry dictates that ϕ is displaced in only one totally symmetric coordinate, so that, $\phi(t)$ tends to return, if in distorted form, to the Franck-Condon region; (3) accidents (rare) occur in which $\langle \phi | \phi(t) \rangle$ returns to the Franck-Condon region in non-obvious way; this can happen if $\phi(0)$ is near a classical periodic orbit with short period. These periodic orbits do exist, even at high energy, where the dynamics is very anharmonic.

From the above description, it should be clear that the more phase space $\phi(t)$ has to rattle around in, the less likely it is to come back any time soon to its birthplace. As we wait longer and longer for $\phi(t)$ to return, we shall have to look on a finer and finer frequency scale to see structure. For this to be true, the gaps between eigenstates that have significant Franck-Condon intensity must get smaller and smaller. In the limit in which $\phi(t)$ can explore the whole phase space available at that energy (stochastic limit), all the Franck-Condon factors not required to be zero by symmetry must have significant intensity. These ideas were the basis for a criterion for detection of stochastic or chaotic motion in a molecule via the spectrum.¹³

Fermi Resonance. Our time-dependent analysis can go far enough to explain the spectral signature of a Fermi resonance which "turns on" only after some threshold energy.¹⁴ Consider a totally symmetric stretch (s) interacting with some non totally symmetric mode (u). The first anharmonic term in the potential that can couple these modes has the form λsu^2 . If, as in many electronic transitions, a high-symmetry molecule retains the same symmetry in the excited state, only s is displaced. Still, energy can flow from s into u. This is permitted since the coupling term λsu^2 has the proper symmetry and can create even overtones in the u-mode at the expense of a quantum of s. If s has twice the frequency of u ($\omega_s = 2\omega_u$), the term λsu^2 is all set to couple s and u directly and strongly. Exactly this happens in the famous Fermi resonance involving the symmetric stretch and the bend in CO₂. The usual splitting and intensity borrowing of levels occurs. But what if $\omega_s \neq 2\omega_u$? It turns out that $\omega_s = \omega_u$, $2\omega_s = 3\omega_u$, $\omega_s = 3\omega_u$, etc., are all resonant also but weaker than the 2:1 resonance when λsu^2 is the coupling term.¹⁴ If the frequency ratio does not involve small integers, the situation is even more interesting, and far more common. Strangely, this more common situation has received little attention.

Let us examine the qualitative features of a Fermi resonance between two initially nonresonant modes. Clearly, larger coupling λ will help couple the two modes in the off-resonant case, as will increased energy (displacement) in s, since this makes λsu^2 effectively a larger term. Thus, the resonance turns on above some threshold in energy. This happens in CHCl₃,¹⁵ where the two modes are the C-H stretch and the C-H bend. The Franck-Condon spectrum shows only weak combination lines near the symmetric stretch overtones below resonance, but the combination lines grow rapidly in intensity above resonance. This occurs at $\nu \approx 6$ in the C-H stretch overtones in CHCl₃. Well above res-

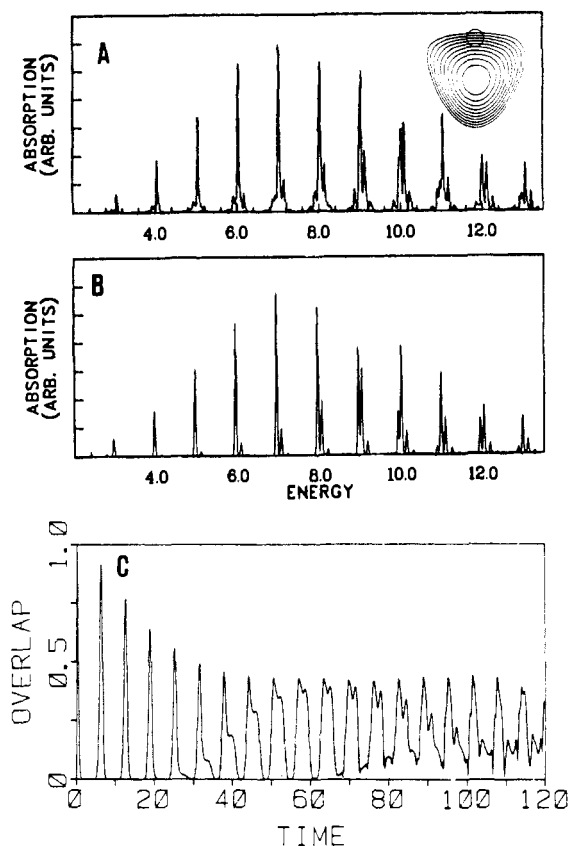


Figure 4. (A) Semiclassical Franck-Condon spectrum for the potential surface and wave packet shown in the inset. (B) Converged quantum mechanical calculation of same. (C) $|\langle \phi | \phi(t) \rangle|$ (quantum), showing T_1 , T_2 , T_3 , and T_4 time scales.

onance, clusters of lines appear near the would-be positions of the pure symmetric stretch overtones.

A close correspondence was shown to exist between the classical and quantum Fermi resonances of this type.¹⁴ The quantum and classical onset energy and the extent of resonance are very similar.

Below, we will describe methods that use classical trajectories to get a complete and accurate molecular spectrum.¹⁶ Applied to Fermi resonances of the type just discussed, we get Figure 4. The spectrum is that of a wave packet displaced along the s coordinate and coupled via λsu^2 to the u coordinate (see the insert in Figure 4A). The numerically converged quantum mechanical basis set calculation is shown in Figure 4B.¹⁴ Note the growth of the Fermi resonant clusters above $E \approx 6.8$, which is a resonance threshold energy. The semiclassical spectrum obtained from the trajectories is shown in Figure 4A.

The onset of Fermi resonance between two modes is separate from the question of the onset of chaotic dynamics of the type that would lead to RRKM behavior, for example. Two modes can be happily in resonance with one another, sharing energy between themselves but not with other modes. The resonant exchange of energy between the modes can occur in a very regular oscillatory fashion.

The function $|\langle \phi | \phi(t) \rangle|$ for the case of Figure 4, A and B, is shown in Figure 4C. At early times, it is similar to the photodissociation case, Figure 2A. All three time scales, T_1 , T_2 , T_3 , can be seen in Figure 4, in addition to a new one T_4 , which occurs at about $T = 40$. This

(13) E. J. Heller, *J. Chem. Phys.*, **72**, 1337 (1980).

(14) E. J. Heller, E. B. Stechel, and M. J. Davis, *J. Chem. Phys.*, **73**, 4720 (1980).

(15) H. L. Fang and R. L. Swofford, *J. Chem. Phys.*, **72**, 6382 (1980).

(16) E. J. Heller, *J. Chem. Phys.*, **75**, 2923 (1981).

new time scale corresponds to the resonant return of energy from the u stretch back to the s stretch. The time $T_4 \approx 40$ should give rise to structure on the frequency scale of $2\pi/40 = 0.15$. This is indeed roughly the splitting between the peaks within the overtone bands seen in Figure 4, A and B. The bandwidths of the overtone clusters is determined by the T_3 decay. This decay is the result of the spreading of $\phi(t)$ out into the u domain, reducing its overlap with ϕ after each successive period in the symmetric coordinate.

Evidently, since only classical trajectories were used to generate Figure 4A, *all four time scales T_1 – T_4 , their underlying dynamics, and their resulting spectral features are essentially classical in nature.*

Raman Scattering. The time-dependent wavepacket description of Raman scattering leads to even more insight and practical utility than the one-photon absorption and emission just discussed. In vibrational Raman scattering, there is a great wealth of information about potential surfaces and dynamics obtained by monitoring the Raman profiles of several final vibrational modes as a function of incident frequency. This will become clear in the examples below. First, let us establish the “usual” Kramer–Heisenberg–Dirac expression and then the time-dependent expression that we prefer.

Suppressing the directional aspects of the transition moments μ , the Raman amplitude to go from the ground vibrational state $|0\rangle$ to the n th vibrational state $|n\rangle$ (assuming a single contributing excited electronic potential surface) is given by the Kramer–Heisenberg–Dirac expression

$$\alpha_{0 \rightarrow n}(\omega) = \sum_k \frac{\langle n | \mu | \psi_k \rangle \langle \psi_k | \mu | 0 \rangle}{E_0 + \hbar\omega - E_k + i\Gamma} + (\text{nonresonant term}) \quad (8)$$

In this expression, ω is the frequency of incident radiation, ψ_k is the k th vibrational eigenstate on the excited surface, and E_k is the energy of that state.

It is often exceedingly impractical to take the KHD equation literally. Depending upon the displacement of the equilibrium position in the excited state, the ψ_k that contribute most may be highly vibrationally excited. For a polyatomic molecule with 6 to 10 or more degrees of freedom, this makes the calculation of the ψ_k essentially impossible. The ψ_k are nonseparable functions of all the internal coordinates of the molecule. No computer, present day or contemplated, could possibly cope with the numerical determination of the ψ_k 's when there are as many as 10^6 eigenstates per wavenumber. This is a common situation. Altogether, billions of levels may contribute to the sum in the KHD expression. Even when there are only a few degrees of freedom and the energies are low enough that the density of states is small, the technology for finding true eigenfunctions of a given potential surface is not well developed. Furthermore, finding these eigenfunctions in the energy regime of the absorption spectrum (the resonant Raman regime) requires knowledge of the potential surface for all configurations appropriate to this regime in energy.

Can Raman scattering really be so complicated? Certainly not; *for large molecules, on or off resonance, a tiny fraction of the excited-state potential surface determines the intensity into a given final state $|n\rangle$,*

and there is no need to know any of the ψ_k 's or E_k 's or any of the matrix elements that appear in eq 8! This is easily seen with the alternate recipe:^{12,17}

$$\alpha_{0 \rightarrow n}(\omega) = \int_0^\infty e^{i\omega t - \Gamma t} \langle \phi_n | \dot{\phi}(t) \rangle dt + (\text{nonresonant term}) \quad (9)$$

where

$$|\phi\rangle = \mu|\chi\rangle, \quad |\phi_n\rangle = \mu|\chi_n\rangle$$

and $\phi(t)$ is the same wavefunction used in the photoabsorption equation (eq 6). The Raman scattering into a given final state n is proportional to the square of the amplitude given in eq 8 or 9.

The procedure for Raman scattering is thus very similar to that for photoabsorption. The same dynamics of the same wavepacket is involved, but it is projected onto different final states rather than onto itself. A half-Fourier integral is also involved. Once we have found $\phi(t)$ by any means, we might as well compute both the absorption and the Raman cross sections, for they are equally easy.

The ingredient $\phi(t)$ is generally vastly easier to calculate than the ψ_k eigenfunctions. After all, we have $\phi(0)$ given to us, and $\phi(t)$ does not become terribly complicated within a few vibrational periods. There are many ab initio ways of finding $\phi(t)$, including time-dependent basis-set variational methods, but we have not particularly pursued these, preferring the semiclassical approach discussed below. The localized wave-packet nature of ϕ and the relatively short times it needs to be propagated virtually cry out for a semiclassical approach.

The integral in eq 9 is on $(0, \infty)$. Why, then, do we claim that only short times are required to evaluate the expression? There are two reasons. Most obvious, one has the phenomenological damping factor Γ in the integrand. This is common practice in Raman scattering (Γ appears in the denominator of the KHD expression) and represents the effect of dephasing due to other degrees of freedom not explicitly included in the wave functions ϕ and ϕ_n . Typically, $1/\Gamma$ corresponds to a few vibrational periods.

Second, and less obvious, is that, if the incident frequency ω is detuned from resonance, an Uncertainty Principle argument holds, $\Delta\omega\tau \approx 1$, where $\Delta\omega$ is the detuning from resonance and τ is interpreted as the lifetime of the wavepacket $\phi(t)$ on the excited state. This was shown by Lee and Heller,¹² and it arises out of a rapid, self-canceling oscillation of the integrand in eq 9 off-resonance. Thus, we can easily perform subpicosecond dynamics on the upper surface by detuning a CW laser from resonance! A beautiful illustration of this is given in Figure 6, explained below. First, let us examine Figure 5, A and B. They show the wavepacket $\phi(t)$ transported temporarily to the upper surface, undergoing dynamics there for a short time (i.e., τ) and coming back down. Both “up” and “down” trips are Franck–Condon; position and momentum are conserved. If the forces in the excited state in the Franck–Condon region are along the x coordinate (Figure 5A), then the x mode will be enhanced and the y mode will not as resonance is approached and $\phi(t)$ lives longer upstairs. This is because $\phi(t)$ is displaced

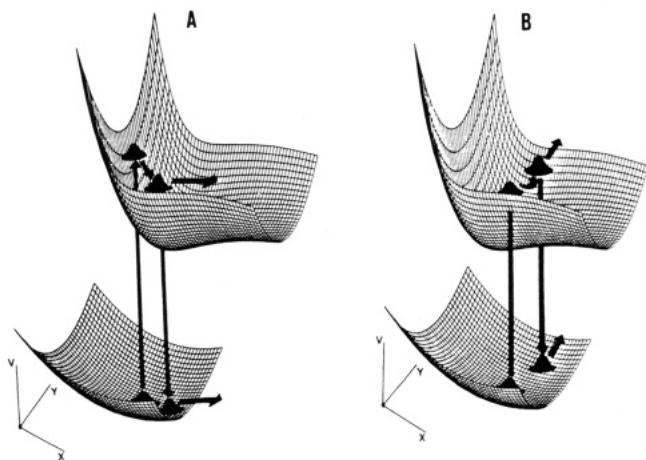


Figure 5. (A) Raman scattering from an upper potential surface, where the wave packet acquires motion in the x direction initially; x -mode overtones will be enhanced in the Raman as resonance is approached. (B) y modes enhanced due to y -motion initially.

during the course of its motion along the x direction, and this, together with the momentum it has acquired, causes it to overlap *excited states* in the x mode once it is back "downstairs". The horizontal arrows indicate the momentum of $\phi(t)$ at the time of its return to the lower surface. If the forces are along the y direction, of course then the y mode is enhanced (Figure 5B). This picture of near-resonant and resonant Raman scattering clearly shows the paramount importance of the Franck-Condon region and that part of the potential surface sampled by $\phi(t)$ in its early motion. Other regions of the potential surface are not important, nor is there any information in the Raman intensities about the potential surface in these regions.

In comparison with the KHD expression, which must "know" the *entire* potential surface covered by the ψ_k 's, a time-dependent version is extremely efficient. Suppose we assume conservatively that a point on the surface has been "explored" by $\phi(t)$ if ϕ reaches 1% of its maximum amplitude there in time t . Then, for 16 degrees of freedom, a Franck-Condon displacement of 0.1 Å, average mass of 12 au, and average frequency of 1000 cm^{-1} , the packet explores less than one part in 10^4 of the surface during the first ten vibrational periods! For a displacement of 0.2 Å, this figure drops to one part in a million. On resonance, ten periods would be a typical time required to define the Raman amplitude to experimental resolution. Off-resonance, as mentioned above, the times can be much shorter. Thus, even with rather small molecules and modest displacements, we stand to gain orders of magnitude in efficiency by using eq 9 instead of eq 8.

A very instructive example is illustrated in Figure 6, which shows ϕ and its early motion on an anharmonic potential surface (inset). A Franck-Condon region was chosen so that the force initially is entirely along the x coordinate. Once the wavepacket has moved somewhat, it also experiences a force along the y axis, and eventually significant y displacement occurs. Our argument about time scales is gratifyingly confirmed in Figure 6, A and B. Below resonance, the wave packet "lives" only for a short time and only x displacement occurs. Notice that the fundamental Raman scattering to the y mode is far below that of the x , both below and above resonance (see Figure 6A). Further, if we delib-

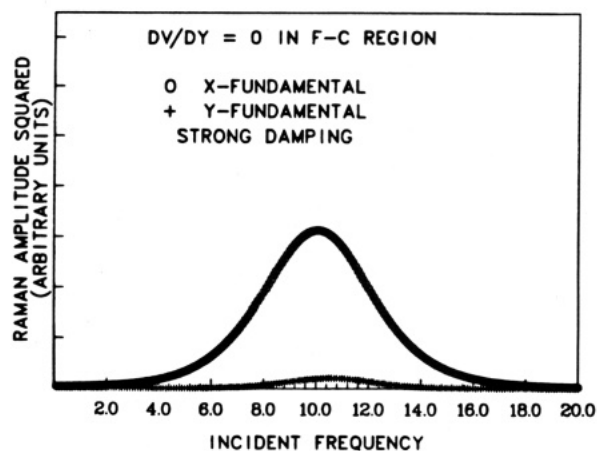
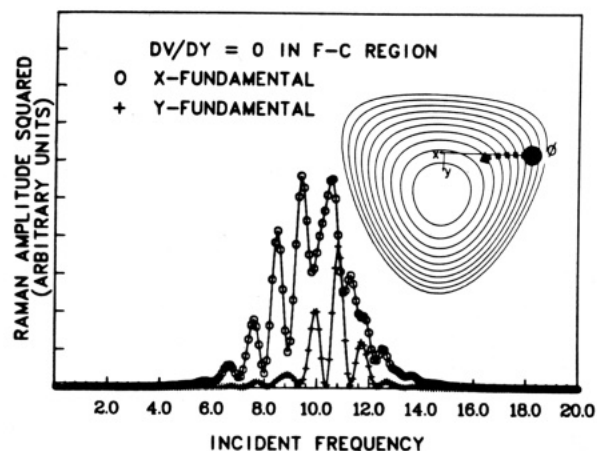


Figure 6. (A) Potential surface, wave-packet ϕ , and the early motion of $\phi(t)$. (Insert) x -mode and y -mode fundamental intensities (0 \rightarrow 1) below, in, and above resonance for moderate damping. (B) Same as (A) except for large damping constant Γ .

erately quench the dynamics on the upper surface by choosing a large Γ , then the y fundamental is drastically quenched relative to the x at all incident frequencies (Figure 6B). This example dramatically illustrates how information about short-time dynamics is contained in the Raman studies.

Short Times and Long Times. Time is of the essence in our semiclassical approach. If spectra are needed to high resolution, the implied times may be too long for an accurate semiclassical determination of $\phi(t)$. All time-dependent semiclassical approximations get worse as time increases. Thus, the semiclassical spectra determined from an autocorrelation function become less trustworthy at higher resolution. If higher resolution information is needed, either we have to introduce variational corrections or we have to invent even better semiclassical methods.

Things are delightfully simple at very short times. And in spite of the simplicity, much can still be learned that is new. For example, a simple formula pertains to the intensity ratio of the fundamentals of two modes in preresonant Raman spectra.¹⁸ It is derived by short-time approximations to the dynamics. For any two modes x and y , we have

(18) E. J. Heller in "Potential Energy Surfaces and Dynamics Calculations", D. C. Truhlar, Ed., Plenum, New York, 1981.

$$\frac{I_{0-1}^y}{I_{0-1}^x} = \frac{\omega_x''}{\omega_y''} \left(\frac{V_y'}{V_x'} \right)^2 \quad (10)$$

where I_{0-1}^y is the Raman intensity into the fundamental of the y mode, ω_y'' is the vibrational frequency at the y mode in the ground state, V_y' is the slope of the upper potential surface in the y direction, evaluated at the equilibrium of the ground state, etc. This remarkably simple formula is proving itself quite accurate for preresonant Raman spectra (just below the 0-0 band in absorption). The formula assumes that the transition moment is a weak function of position. Remembering the $\Delta\omega\tau = 1$ arguments, the fact that the ratio of intensities depends only on the immediate Franck-Condon region squares with the notion of short-time dynamics, in the preresonance frequency domain.

Semiclassical Methods. While the physical picture of wave-packet dynamics for molecular spectroscopy is appealing, and the short-time analytical results such as eq 10 are useful, we still need a reliable means for the numerically propagating wave packets $\phi(t)$ for many (anharmonic) degrees of freedom. We have described such methods in the literature.^{10,11} They rely upon the flexible properties of Gaussian wave packets. Basically, three steps are involved. (1) Expansion of $\phi(0) \equiv \phi$ in terms of complex Gaussians g_i ; i.e., $\phi = \sum_i c_i g_i$. This is an accurate and well-defined procedure. (2) Propagation of the g_i individually. This is accomplished in wholly classical fashion; i.e., trajectories determine every possible parameter in the Gaussian: $\phi(t) = \sum_i c_i g_i(t)$, and projection of $\phi(t)$ onto ϕ in some other state, as the spectroscopy dictates. These projections only involve overlaps between Gaussians. (3) Superposition of the Gaussians (according to the coefficients c_i) to form $\phi(t)$, projection onto ϕ (the overlaps are all Gaussian in form), and Fourier transform.

Raman and absorption spectra calculations on semiempirical potential surfaces of up to 33 degrees of freedom have been carried out successfully using our wave-packet technique.¹⁷

The propagation takes place at various levels of sophistication. The simplest method is the frozen Gaussian approximation (FGA),¹⁶ wherein the Gaussian packets rigidly follow a guiding classical trajectory. The next level of accuracy is the "thawed" Gaussian approximation (TGA),^{10,11} in which the Gaussians are allowed to distort as time evolves. Finally, we can allow the coefficient c_i to vary with time according to a time-dependent variational principle,⁵ using the thawed (or frozen) Gaussians as a basis set. This is (in principle) an ab initio technique capable of numerical convergence.

We have used the wave packets for a host of other purposes not emphasized in this short review. These include photodissociation,^{9-11,19} criteria for the onset of stochasticity,¹³ as a "phase-space" basis set in standard matrix diagonalization,²⁰ and the investigation of local modes and dynamical tunneling.²¹⁻²³ Ongoing developments of the method include incorporation of rotations, finite-temperature spectra, and spectra in the

presence of nonadiabatic curve crossings.

Conclusion

In a certain sense, vibrational dynamics has lagged behind electronic structure calculations in that it has lacked simple, low-level methods analogous to Hartree-Fock, or Hückel theory, etc. That is, it has lacked an intuitive and practical set of tools to treat "real" molecules with many degrees of freedom, high energies, and high density of states. (Perturbation and variational methods are well developed for vibrational spectroscopy of small molecules at low energies.²⁴) The classical S-matrix methods²⁵ and quasi-classical methods so important for scattering and unimolecular dynamics^{26,27} seem not to have previously developed counterparts for bound-state dynamics and spectroscopy. We are developing a new set of tools for molecular spectroscopy of bound states and photodissociation. The dynamics and many spectral features resulting from a given potential surface are now calculated with enough ease that ab initio and semiempirical theorists of electronic structure can look more often to the dynamicists for the experimental implications of their calculations.

The time-dependent wave-packet formulation of spectroscopy offers intuitive and computational assistance in several traditional fields of chemistry. For absorption spectra, the method could be called a Franck-Condon analysis without Franck-Condon factors.²⁸ For example, a photochemist interested in shifts in shape, maxima, and width of electronic absorption bands as a function of solvent or structural changes can understand these shifts in terms of changes in very local properties of the ground and excited potential surfaces in the Franck-Condon region. Our methods also strongly suggest preresonance and resonance Raman spectroscopy as additional probes of such properties.

The wave-packet picture further aids the photochemist if we follow it for longer times: Does the bond that breaks result forthwith from dynamics starting in the Franck-Condon region, or is intra- or intermolecular energy transferred (corresponding to a less direct classical dissociative path)? If an internal conversion is required before dissociation, does the wavepacket dynamics lead to regions where radiationless coupling is more favorable? After the dissociation, what is the distribution of energy among the fragments? All these questions are naturally formulated and answered in a time-dependent framework.

I am indebted to my students and postdoctoral research fellows (M. J. Davis, D. J. Tannor, R. C. Brown, Dr. S.-Y. Lee, and Dr. E. B. Stechel), who worked on and made possible the research described here. For inspiration derived from their work and for helpful conversations, I wish to thank the students and postdoctorals mentioned above and my colleagues K. C. Kulander, W. H. Miller, R. Harris, R. A. Marcus, R. Pack, R. Walker, R. Wyatt, K. R. Wilson, M. S. Child, and M. V. Berry. The work described here was performed with the help of NSF Grant CHE-80-16908, the Sloan Foundation, and the Dreyfus Foundation. Part of the research and the writing of this Account was performed while I was with the T-12 Group at Los Alamos National Laboratory.

(19) R. C. Brown and E. J. Heller, *J. Chem. Phys.*, **75**, 186 (1981).

(20) M. J. Davis and E. J. Heller, *J. Chem. Phys.*, **71**, 3383 (1979).

(21) E. J. Heller and M. J. Davis, *J. Phys. Chem.*, **85**, 307 (1981).

(22) M. J. Davis and E. J. Heller, *J. Chem. Phys.*, **75**, 246 (1981).

(23) R. T. Lawton and M. S. Child, *Mol. Phys.*, **37**, 1779 (1979); **40**, 733 (1980).

(24) See, e.g., G. D. Carney, *Adv. Chem. Phys.*, **37**, 305 (1978).

(25) See, e.g., W. H. Miller, *Adv. Chem. Phys.*, **25**, 69 (1974).

(26) See, e.g., D. L. Bunker, *Methods Comput. Phys.*, **10**, 287 (1971).

(27) W. L. Hase in "Potential Energy Surface and Dynamics Calculations", D. G. Truhlar, Ed., Plenum Press, New York, 1981.

(28) J. I. Zink and E. J. Heller, to be published.